

See discussions, stats, and author profiles for this publication at: <https://www.researchgate.net/publication/11449039>

Naked Clusters of 56 Tin Atoms in the Solid State

ARTICLE *in* JOURNAL OF THE AMERICAN CHEMICAL SOCIETY · MAY 2002

Impact Factor: 12.11 · DOI: 10.1021/ja012549j · Source: PubMed

CITATIONS

20

READS

13

2 AUTHORS, INCLUDING:



Svilen Bobev

University of Delaware

257 PUBLICATIONS 2,035 CITATIONS

SEE PROFILE

Naked Clusters of 56 Tin Atoms in the Solid State

Svilen Bobev and Slavi C. Sevov*

Contribution from the Department of Chemistry and Biochemistry, University of Notre Dame,
Notre Dame, Indiana 46556

Received November 15, 2001

Abstract: Isolated, gigantic tin clusters of 56 atoms are discovered in the ternary compound $\text{Ba}_{16}\text{Na}_{204}\text{Sn}_{310}$ (cubic, $F\bar{4}3m$, $Z = 1$, $a = 25.2041(8)$ Å) made by direct fusion of the elements at 800 °C. The cluster, made of four face-fused pentagonal dodecahedra, has 36 pentagonal faces and 90 edges, and resembles a concave fullerene “dented” at four places. It is made of three- and four-bonded tin atoms and is “stuffed” with four barium cations, $[\text{Ba}_4@\text{Sn}_{56}]^{36-}$. This is the largest main group naked cluster in the solid state besides the fullerenes. Also occurring in the structure are two other isolated clusters of tin, Sn_{16-n} ($n = 0, 1, 2, 3$, or 4) and Sn_8 .

Introduction

The number of newly discovered main group naked clusters in the solid state has grown immensely in recent years. Many large deltahedral clusters of group 13 were characterized during that time.¹ Lately, the interest has shifted toward group 14 for which cluster formation has been studied only in solutions and in compounds crystallized from them. Known from such solutions are deltahedral *nido*-clusters of Tt_9^{4-} , where Tt (Tetrel) = Ge, Sn, or Pb.¹ Recent studies revealed that the same nine-atom clusters Tt_9^{4-} exist also in “neat” solids with compositions A_4Tt_9 and $\text{A}_{12}\text{Tt}_{17}$, where A = alkali metal.² This breakthrough catalyzed the search for other discrete cluster species in the solid state and led to the discovery of the *arachno*-clusters of Sn_8^{6-} in pseudobinary compounds with mixed alkali metals, $\text{K}_4\text{Li}_2\text{Sn}_8$ and $\text{Rb}_4\text{Li}_2\text{Sn}_8$,³ and the extra-large clusters of Ge_{12}^{12-} and Sn_{12}^{12-} with the shape of truncated tetrahedra in RbLi_7Ge_8 and $(\text{Ca or Sr})\text{Na}_{10}\text{Sn}_{12}$, respectively.^{4,5} Here we describe a phenomenal gigantic cluster of tin found in the mixed-cation compound, $\text{Ba}_{16}\text{Na}_{204}\text{Sn}_{310}$. It is made of 56 tin atoms, Sn_{56} , and has 36 pentagonal faces and 90 edges. The cluster is stuffed with four barium cations, $\text{Ba}_4@\text{Sn}_{56}$, and can be viewed either as made of four fused pentagonal dodecahedra or as a concave bucky ball. The existence of a cluster of tin of this size is indeed unexpected, especially when taking into account that the next largest cluster in this group (besides the carbon fullerenes) is only of 12 atoms, Sn_{12} and Ge_{12} .^{4,5} Molecular chemistry, on the other hand, has produced even larger main-group clusters but as protected with various external ligands. Thus, multishell-like clusters of 69, 77, and 84

aluminum or gallium atoms can be stabilized by amido ligands such as $\text{N}(\text{SiMe}_3)_2$ that bond covalently to the outer atoms of the corresponding clusters $[\text{Al}_{69}\{\text{N}(\text{SiMe}_3)_2\}_{18}]^{3-}$, $[\text{Al}_{77}\{\text{N}(\text{SiMe}_3)_2\}_{20}]^{2-}$, and $[\text{Ga}_{84}\{\text{N}(\text{SiMe}_3)_2\}_{20}]^{4-}$.⁶

Experimental Section

Synthesis. All manipulations were performed in an inert atmosphere glovebox (moisture level below 1 ppm). The new compound $\text{Ba}_{16}\text{Na}_{204}\text{Sn}_{310}$ was synthesized by direct reaction of the elements at high temperature. The surfaces of Na (ingot, Alfa, 99.9%, sealed under Ar) and Ba (rod, Alfa, 99.2%, sealed under Ar) were cleaned off with a scalpel immediately before use, while Sn (rod, Alfa, 99.999%) was used as received. All reactions were carried out in niobium tubular containers that were sealed by arc-welding. These containers were in turn jacketed in silica ampules that were then evacuated and flame-sealed.

Initially, $\text{Ba}_{16}\text{Na}_{204}\text{Sn}_{310}$ was synthesized as the major product of a reaction loaded as $\text{Ba}_{1.5}\text{Na}_{10}\text{Sn}_{23}$. It was intended to produce a barium version of the recently reported layered clathrate derivatives $\text{A}_3\text{Na}_{10}\text{Sn}_{23}$ (A = K, Rb, Cs).⁷ This reaction was carried out at 950 °C for 48 h and cooled to room temperature with a rate of 5 °C/h. (Ba has the highest melting point at 725 °C, while the Ba–Sn phase diagram is unknown and the highest melting point in the Na–Sn diagram is about 580 °C.) Found in the product of this reaction were also traces of BaSn_3 and NaSn as well as unreacted Sn metal (est. total mass fraction of less than ca. 10%). Later, when the structure of $\text{Ba}_{16}\text{Na}_{204}\text{Sn}_{310}$ was refined and the approximate composition determined from single-crystal X-ray diffraction work, the compound was synthesized in high yields from reactions with atomic ratios Ba:Na:Sn = 1:(10–13):(19–22). These mixtures were heated at 800 °C for 2 weeks and were then slowly cooled to room temperature with a rate of 2 °C/h. None of them, however, produced $\text{Ba}_{16}\text{Na}_{204}\text{Sn}_{310}$ as a single phase. Another set of mixtures of the same compositions was prepared, and these were melted at 1000 °C for 12 h, quenched to 0 °C in ice–water, annealed at 300 °C for 2 weeks, and then slowly cooled to room temperature with a

- (1) (a) Corbett, J. D. *Chem. Rev.* **1985**, 85, 383. (b) Corbett, J. D. *Struct. Bonding* **1997**, 87, 157. (c) Nesper, R. *Angew. Chem., Int. Ed. Engl.* **1991**, 30, 789. (d) Corbett, J. D. *Angew. Chem., Int. Ed.* **2000**, 39, 670.
- (2) (a) Quenéau, V.; Sevov, S. C. *Angew. Chem., Int. Ed. Engl.* **1997**, 36, 1754. (b) Quenéau, V.; Sevov, S. C. *Inorg. Chem.* **1998**, 37, 1358. (c) Quenéau, V.; Todorov, E.; Sevov, S. C. *J. Am. Chem. Soc.* **1998**, 120, 3263. (d) Todorov, E.; Sevov, S. C. *Inorg. Chem.* **1998**, 37, 3889.
- (3) Bobev, S.; Sevov, S. C. *Angew. Chem. Int. Ed.* **2000**, 39, 4108.
- (4) Bobev, S.; Sevov, S. C. *Angew. Chem. Int. Ed.* **2001**, 40, 1507.
- (5) Bobev, S.; Sevov, S. C. *Inorg. Chem.* **2001**, 40, 5361.

- (6) (a) Ecker, A.; Weckert, E.; Schnöckel, H. *Nature* **1997**, 387, 379. (b) Schnepf, A.; Schnöckel, H. *Angew. Chem., Int. Ed.* **2001**, 40, 712. (c) Köhnlein, H.; Purath, A.; Klemp, C.; Baum, E.; Krossing, I.; Stösser, G.; Schnöckel, H. *Inorg. Chem.* **2001**, 40, 4830.
- (7) Bobev, S.; Sevov, S. C. *Inorg. Chem.* **2000**, 39, 5930.

rate of 5 °C/h. They did not provide a single-phase product either, but the crystallinity of $\text{Ba}_{16}\text{Na}_{204}\text{Sn}_{310}$ was orders of magnitude better than the other syntheses. This allowed easy phase separation of the large crystals of the new compound from the powderish other phases. Such pure samples of selected crystals were used for magnetic measurements and elemental analysis.

The outcome of all reactions was monitored by X-ray powder diffraction. Since $\text{Ba}_{16}\text{Na}_{204}\text{Sn}_{310}$ is air-sensitive, the samples are prepared inside the glovebox by placing the powder between two pieces of Scotch tape. The diffraction experiment was carried out in an evacuated Enraf-Nonius Guinier camera with a vacuum chamber (Cu $K\alpha_1$ radiation, $\lambda = 1.540562$ Å). A least-squares refinement of the measured 2θ values relative to those of NBS (NIST) silicon as an internal standard verified the lattice constants obtained from the single-crystal work. The lattice parameters of the compound made by the different reactions were virtually identical, and this suggested that the compound is a line compound (or with negligible stoichiometry breadth). This was corroborated by the virtually identical compositions of the refined structures of three different single crystals from different reactions (see below). It was confirmed further by the results of elemental analysis carried out by the ICP method (see below).

Structure Determination. Several single-crystal X-ray diffraction data sets were acquired for different crystals of $\text{Ba}_{16}\text{Na}_{204}\text{Sn}_{310}$ selected from different reactions. These were collected both on Enraf-Nonius CAD4 and BRUKER APEX-CCD diffractometers with graphite monochromated Mo $K\alpha$ radiation ($\lambda = 0.71073$ Å) at various temperatures. The crystals were selected inside the glovebox and were sealed in thin-walled glass capillaries. The structure was solved by direct methods and the different data sets were refined on F^2 with the aid of the SHELXTL-V5.1 software package. The specifics of the structure determinations of the different data sets are discussed next.

Initially, an octant of diffraction data was collected (CAD4, ω - 2θ scans, $2\theta_{\text{max}} = 50^\circ$) on a crystal ($0.12 \text{ mm} \times 0.12 \text{ mm} \times 0.10 \text{ mm}$) selected from the first sample (Ba:Na:Sn = 1.5:10:23). The total of 2013 reflections were corrected for absorption with the aid of the average of 3 ψ -scans at different θ angles ($R_{\text{int}} = 0.048$; $T_{\text{min}}/T_{\text{max}} = 0.306/0.358$). The observed extinction conditions and the intensity statistics were consistent with the acentric $F\bar{4}3m$ space group. Direct methods in this space group provided seven peaks with distances to each other that were appropriate for tin atoms, and they were so assigned. One of the remaining six peaks was assigned as Ba based on its height and distances, while the other five were assigned as sodium atoms. A few least-squares refinement cycles confirmed the correct choice of the space group and the proper assignment of the atoms. In essence, the major part of the structure was deduced at this stage, but the difference Fourier map revealed five remaining peaks of moderate-to-low intensity. These were assigned as two Sn and three Na atoms. The subsequent isotropic refinement led to $R1 \approx 12\%$ and a virtually flat difference Fourier map. However, the two tin and three sodium positions that were added last showed abnormally large thermal parameters. When refined as anisotropic they became extremely elongated which suggested either some sort of disorder or, perhaps, too high symmetry of the space group and possible twinning. To check the latter presumption, collected on the BRUKER CCD diffractometer at -173 °C was a full sphere of data on the same crystal. Special attention was paid to the symmetry and the lattice parameters as well as the data integration in the correct Bravais lattice. Careful and systematic examination of the reciprocal lattice confirmed the F -centering, and the same cubic unit cell was indexed and refined based on 9607 reflections ($I > 10\sigma I$). The total of 35957 reflections were readily merged in the same acentric space group, $F\bar{4}3m$ ($R_{\text{int}} \approx 0.06$). However, the subsequent structure refinement using this data set showed the same problems and did not improve the overall result. The problematic tin atoms were still with large thermal parameters despite the much lower temperature. The low-temperature data revealed also small and diffuse electron density around the problematic atoms which

Table 1. Selected Data Collection and Refinement Parameters for $\text{Ba}_{16}\text{Na}_{204}\text{Sn}_{310}$

| | |
|--|---|
| chemical formula | $\text{Ba}_{16}\text{Na}_{204}\text{Sn}_{310.0(8)}$ |
| formula weight | 43675.37 |
| space group, Z | $F\bar{4}3m$ (No. 216), 1 |
| unit cell parameters | $a = 25.2041(8)$ Å $V = 16010.8(9)$ Å ³ |
| radiation, λ (Å) | Mo $K\alpha$, 0.71073 |
| $\mu(\text{cm}^{-1})$ | 129.40 |
| $\rho_{\text{calc}}(\text{g/cm}^3)$ | 4.530 |
| R indices ($I > 2\sigma I$) ^a | $R1 = 3.54\%$, $wR2 = 10.14\%$ |
| R indices (all data) | $R1 = 3.62\%$, $wR2 = 10.24\%$ |

$$^a R1 = \sum |F_o| - |F_c| / \sum |F_o|; wR2 = [\sum [w(F_o^2 - F_c^2)^2] / \sum [w(F_o^2)^2]]^{1/2}; w = 1/[\sigma^2 F_o^2 + (0.0669P)^2 + 517.12P], P = (F_o^2 + 2F_c^2)/3.$$

pointed to statistical disorder as the most likely reason for the problems. Nevertheless, extensive and systematic analysis was carried out for possible lower-symmetry space group. Unsuccessful attempts to better refine the structure were made in $F432$, $F23$, $R3m$, $R3$, and even in $P1$. The trigonal cases were refined as twinned multiple crystals along the four body diagonals of the cubic cell combined with merohedral twinning. The absolute structure was confirmed based on more than 900 measured Friedel pairs, more than 80% of all possible. No noticeable violations of the Friedel's law were observed. This suggested that the problems in the structure refinement were most likely associated with statistical disorder rather than anomalous scattering or merohedral twinning.

Additional X-ray diffraction data sets were collected on two more single crystals that were selected from reactions loaded with different compositions and carried out at different temperature profiles. For one of them ($0.12 \text{ mm} \times 0.10 \text{ mm} \times 0.08 \text{ mm}$, selected from a reaction loaded as Ba:Na:Sn = 1:10:20 and run at 800 °C for two weeks) an octant of diffraction data was collected at room temperature on the CAD4 diffractometer with ω - 2θ scans and up to $2\theta_{\text{max}}$ limit of 60° . The total of 6172 collected reflections were corrected for absorption with the aid of the average of 4 ψ -scans at different θ angles ($R_{\text{int}} = 0.053$; $T_{\text{min}}/T_{\text{max}} = 0.306/0.425$). For the second crystal ($0.14 \text{ mm} \times 0.12 \text{ mm} \times 0.12 \text{ mm}$; selected from a reaction loaded as Ba:Na:Sn = 1:12:25; heated at 1000 °C for 12 h, quenched at 0 °C, annealed at 300 °C for 2 weeks, and slowly cooled to room temperature at a rate of 5 °C/h) a full sphere of data was collected at room temperature on the BRUKER CCD (the total of 44496 reflections were corrected for absorption with the aid of the SADABS program, $R_{\text{int}} = 0.027$; $T_{\text{min}}/T_{\text{max}} = 0.265/0.306$). The refinement of this last data set provided the best structural parameters and residuals, and the discussion of the structure from hereafter is based on that structure determination. Details of the data collection and refinement are summarized in Table 1, while the final positional and equivalent isotropic displacement parameters and important distances are listed in Tables 2 and 3, respectively.

In the final refinement one tin position was refined as a split position (Sn7A and Sn7B) while four other sites (Sn6, Sn8, Sn9, Sn10) were refined as partially occupied. Two of the three different clusters in the structure (see Results and Discussion) have such partially occupied or split sites. The sums of the occupancies of the positions of these two clusters labeled as Sn₈ and Sn_{16-n} refined as 8.0(2) and 13.5(1), respectively. Thus, the formula of the compound was refined as $\text{Ba}_{16}\text{Na}_{204}\text{Sn}_{310.0(8)}$. The final residuals were $R1/wR2 = 3.62/10.24\%$ for all 1981 unique reflections and 95 variables.

Elemental Analysis. It is important to point out that the refined compositions of the compound from all refinements of the structure (based on the data sets collected at different temperatures with different machines and on different crystals selected from different reactions), were virtually identical, within 2σ of each other and from $\text{Ba}_{16}\text{Na}_{204}\text{Sn}_{310.0(8)}$. Furthermore, the unit cell dimensions determined from the different room-temperature data sets, 25.2029(6), 25.2041(8), and 25.1998(6) Å were within 5σ of each other. This confirmed that: (a) the compound is a line compound, and b) the stoichiometry is indeed

Table 2. Atomic Coordinates and Equivalent Isotropic Displacement Parameters for Ba₁₆Na₂₀₄Sn₃₁₀.

| atom | site | x | y | z | U _{eq} |
|-------------------|------|------------|------------|------------|-----------------|
| Sn1 | 16e | 0.04891(4) | x | x | 0.0330(3) |
| Sn2 | 16e | 0.82116(4) | x | x | 0.0463(4) |
| Sn3 | 48h | 0.04060(3) | x | 0.16324(4) | 0.0316(2) |
| Sn4 | 48h | 0.11093(3) | x | 0.75627(4) | 0.0426(2) |
| Sn5 | 96i | 0.49836(3) | 0.21600(3) | 0.63489(3) | 0.0371(2) |
| Sn6 ^a | 16e | 0.5763(1) | x | x | 0.049(2) |
| Sn7A ^a | 48h | 0.45976(7) | x | 0.3790(1) | 0.0660(9) |
| Sn7B ^a | 96i | 0.0596(5) | 0.4725(5) | 0.1079(5) | 0.0660(9) |
| Sn8 ^a | 16e | 0.1964(1) | x | x | 0.130(7) |
| Sn9 ^a | 16e | 0.3046(1) | x | x | 0.15(1) |
| Sn10 ^a | 96i | 0.248(1) | 0.3013(3) | 0.1700(3) | 0.20(1) |
| Ba1 | 16e | 0.90420(3) | x | x | 0.0369(3) |
| Na1 | 4b | 1/2 | 1/2 | 1/2 | 0.019(2) |
| Na2 | 16e | 0.6853(7) | x | x | 0.12(1) |
| Na3 | 16e | 0.1302(4) | x | x | 0.075(4) |
| Na4 | 24f | 0.2747(6) | 0 | 0 | 0.23(2) |
| Na5 | 24g | 0.5822(5) | 1/4 | 1/4 | 0.069(3) |
| Na6 | 24g | 0.0612(7) | 1/4 | 1/4 | 0.076(4) |
| Na7 | 48h | 0.1013(2) | x | 0.2839(3) | 0.063(2) |
| Na8 | 48h | 0.1549(3) | x | 0.5312(5) | 0.083(3) |

^a Sn(6), Sn(7A), Sn(7B), Sn(8), Sn(9), and Sn(10) are occupied 41(1), 75(1), 25(1), 49(2), 44(3), 17(1) %, respectively.

very close to Ba₁₆Na₂₀₄Sn_{310.0(8)}. The latter was further corroborated by the elemental analysis carried out by ICP on a Perkin-Elmer Plasma 400 Emission Spectrometer (40 MHz free-running ICP generator and Ar-coiled coil). For that purpose, crystals of Ba₁₆Na₂₀₄Sn₃₁₀ from two different syntheses (those which provided large crystals, see the Synthesis section) were carefully selected under microscope and were dissolved in diluted acid. Prepared were several solutions of different concentrations as well as standards for the elements for four known concentrations. Multiple measurements gave the following weight percents for the elements: 4.88 for Ba, 10.08 for Na, and 85.04 for Sn. The theoretically calculated values based on the formula Ba₁₆Na₂₀₄Sn₃₁₀ are: 5.03 for Ba, 10.74 for Na, and 84.23 for Sn. Considering the accuracy of the ICP method these numbers are in excellent agreement.

Magnetic Measurements. The magnetizations of different samples of Ba₁₆Na₂₀₄Sn₃₁₀ were measured on a Quantum Design MPMS SQUID magnetometer at a field of 3 T over the temperature range 10–280 K. Measurements at lower fields (50, 100 and 300 G) at lower temperatures (down to 4 K) were carried out as well. The samples were made of relatively large crystals of Ba₁₆Na₂₀₄Sn₃₁₀ selected under microscope to achieve nearly single-phase specimens. They were enclosed between quartz rods in a tightly fitting quartz tubing that was sealed at both ends. The raw data were corrected for the holder contribution and for the ion-core diamagnetism. The corrected magnetic susceptibility is temperature-independent and very close to zero between 2.27×10^{-4} and 2.40×10^{-4} emu/mol (average of several measurements on different samples). This is consistent with some electron delocalization, perhaps some electron population of the conduction band.

Results and Discussion

The structure of the new compound Ba₁₆Na₂₀₄Sn₃₁₀ contains three different isolated clusters made of 56, 16, and 8 tin atoms as shown in Figure 1. The first one, Sn₅₆, is the second largest discrete and naked cluster, in terms of number of atoms, of a main-group element after the carbon fullerenes and, with a diameter of about 15 Å, is perhaps the largest in size (Figure 2). It is made of four pentagonal dodecahedra that are fused to each other by sharing faces. The dodecahedra are positioned at the corners of a tetrahedron, and thus, each shares a face with each of the other three dodecahedra. This means that one vertex

Table 3. Important Distances (Å) in Ba₁₆Na₂₀₄Sn₃₁₀

| within Sn ₅₆ | | | cations | | |
|---------------------------|----------|-----------|---------|-----------|-----------|
| Sn1 — | 3 × Sn3 | 2.897(1) | Ba1 — | 3 × Sn1 | 4.012(1) |
| | Na3 | 3.55(2) | | Sn2 | 3.625(2) |
| Sn2 — | 3 × Ba1 | 4.012(1) | | 6 × Sn3 | 4.0797(8) |
| | 3 × Sn4 | 2.921(1) | | 3 × Sn4 | 3.767(1) |
| | 3 × Na2 | 3.43(2) | | 6 × Sn5 | 3.9725(8) |
| | 3 × Na5 | 3.52(1) | Na1 — | 4 × Sn6 | 3.329(4) |
| | Ba1 | 3.625(2) | | 12 × Sn7A | 3.369(2) |
| Sn3 — | Sn1 | 2.897(1) | or | 12 × Sn7B | 3.18(1) |
| | Sn3 | 2.894(2) | Na2 — | 3 × Sn2 | 3.43(2) |
| | 2 × Sn5 | 2.9239(8) | | 3 × Sn4 | 3.20(1) |
| | Na3 | 3.30(1) | | 3 × Na5 | 3.48(1) |
| | Na4 | 3.16(1) | | 3 × Na8 | 4.03(3) |
| Sn4 — | 2 × Ba1 | 4.0797(8) | Na3 — | Sn1 | 3.55(2) |
| | Sn2 | 2.921(1) | | 3 × Sn3 | 3.30(1) |
| | 2 × Sn5 | 2.9054(9) | | Sn8 | 2.98(2) |
| | Na2 | 3.20(1) | | 2 × Sn10 | 3.67(3) |
| | 2 × Na5 | 3.583(3) | | 3 × Na7 | 4.01(1) |
| | 2 × Na8 | 3.434(7) | Na4 — | 2 × Sn3 | 3.16(1) |
| Sn5 — | Ba1 | 3.767(1) | | 2 × Sn7A | 3.00(1) |
| | Sn3 | 2.9239(8) | or | 2 × Sn7B | 3.39(2) |
| | Sn4 | 2.9054(9) | | 2 × Na7 | 3.618(8) |
| | Sn5 | 2.891(1) | Na5 — | 2 × Sn2 | 3.52(1) |
| | Na5 | 3.643(8) | | 4 × Sn4 | 3.583(3) |
| | Na6 | 3.415(8) | | 4 × Sn5 | 3.643(8) |
| | Na7 | 3.221(5) | | 2 × Na2 | 3.48(1) |
| | Na8 | 3.376(8) | | Na6 | 3.61(2) |
| | Ba1 | 3.9725(8) | | 2 × Na8 | 3.63(1) |
| within Sn _{16-n} | | | Na6 — | 4 × Sn5 | 3.415(8) |
| Sn6 — | 6 × Sn7A | 3.273(2) | | Sn10 | 3.03(2) |
| | Na1 | 3.329(4) | | 4 × Na7 | 3.974(6) |
| | 3 × Na8 | 3.024(1) | Na7 — | 2 × Sn5 | 3.221(5) |
| Sn7A — | 2 × Sn6 | 3.273(2) | | Sn7A | 3.24(1) |
| | Sn7A | 2.869(5) | or | Sn7B | 3.46(2) |
| | 2 × Sn7A | 2.876(5) | | Sn9 | 3.394(9) |
| | Na1 | 3.369(2) | | Sn10 | 3.11(1) |
| | Na4 | 3.00(1) | | Na3 | 4.01(1) |
| | Na7 | 3.24(1) | | 2 × Na6 | 3.974(6) |
| | 2 × Na8 | 3.51(1) | | 2 × Na8 | 3.92(2) |
| Sn7B — | Sn7B | 2.86(2) | Na8 — | 2 × Sn4 | 3.434(7) |
| | Sn7A | 2.95(1) | | 2 × Sn5 | 3.376(8) |
| | Sn7A | 3.06(1) | | Sn6 | 3.02(1) |
| | Na1 | 3.19(1) | | 2 × Sn7A | 3.51(1) |
| | Na4 | 3.39(2) | or | 2 × Sn7B | 3.06(2) |
| | Na7 | 3.46(2) | | Na5 | 3.63(1) |
| | Na8 | 3.06(2) | | 2 × Na7 | 3.92(2) |
| within Sn ₈ | | | | Na8 | 4.03(3) |
| Sn8 — | 2 × Sn9 | 2.729(5) | | | |
| | 2 × Sn10 | 3.02(1) | | | |
| | Na3 | 2.98(2) | | | |
| Sn9 — | 2 × Sn8 | 2.729(5) | | | |
| | 2 × Sn10 | 3.10(2) | | | |
| | 3 × Na7 | 3.394(9) | | | |
| Sn10 — | Sn8 | 3.02(1) | | | |
| | Sn9 | 3.10(2) | | | |
| | Sn10 | 2.76(5) | | | |
| | Na3 | 2.94(4) | | | |
| | Na6 | 3.67(3) | | | |
| | Na7 | 3.03(2) | | | |
| | Na7 | 3.11(1) | | | |

would be common for all four dodecahedra, the one that belongs to a shared pentagonal face for each dodecahedron. However, in this particular case, this vertex is missing, and the center of Sn₅₆ is empty (Figure 2b). Due to small distortions in the dodecahedra from the ideal *I_h* symmetry, this central position becomes unrealistically close to the other tin atoms of the cluster at a distance of 2.1 Å.

The Sn₅₆ cluster has 36 pentagonal faces and 90 edges and carries the full *T_d* symmetry of the *F43m* space group. It is made of five crystallographically unique tin atoms, Sn1 to Sn5 (Figure 2), with Sn–Sn distances that fall in a narrow range, 2.891–(1)–2.9239(8) Å (Table 3). These distances compare very well with other localized single-bond distances such as those of the

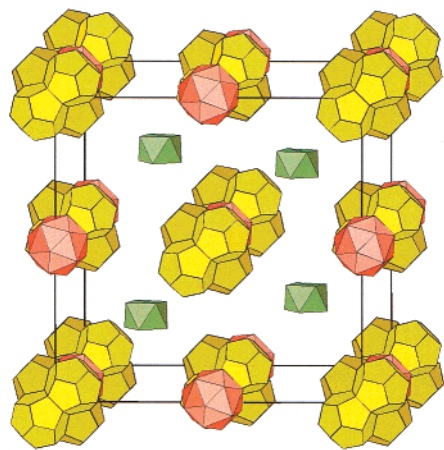


Figure 1. Schematic polyhedral view of the *fcc* cell of $\text{Ba}_{16}\text{Na}_{204}\text{Sn}_{310}$. For the purpose of clarity all clusters are shown smaller than actual size, and all cations are omitted. The largest of the clusters, Sn_{56} shown in yellow, forms the close-packed lattice (corners and face centers), while Sn_{16-n} (red) and Sn_8 (green) occupy the octahedral and half of the tetrahedral holes, respectively.

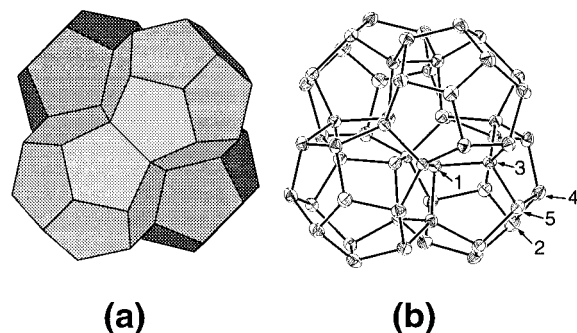


Figure 2. Closer (a) polyhedral and (b) ORTEP (thermal ellipsoids at 75% probability level) views of the giant isolated cluster Sn_{56} in $\text{Ba}_{16}\text{Na}_{204}\text{Sn}_{310}$. The cluster is made of four face-fused pentagonal dodecahedra and has 56 vertexes, 36 pentagonal faces, and 90 edges. It carries the full T_d symmetry of the $F\bar{4}3m$ space group. The central atom that would be common for all four dodecahedra is missing. The majority of the tin vertexes (their numbers are given in b) are three-bonded but 12 of them (Sn_3) are four-bonded.

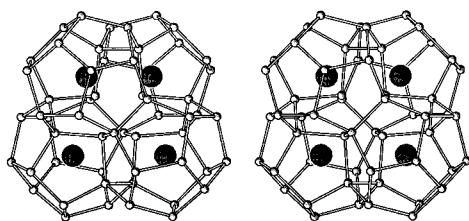


Figure 3. Stereoview of Sn_{56} with the four endohedral barium cations shown.

Sn_4^{4-} tetrahedra and the truncated tetrahedra of Sn_{12}^{12-} , but are shorter, as might be expected, than the distances in species with delocalized bonding such as the deltahedral clusters Sn_9^{4-} and Sn_8 .^{6–3,5,8} Twelve of the 56 tin atoms (Sn_3), those that are shared between dodecahedra, are four-bonded while the other 44 are three-bonded (Figures 2 and 3). The number of bonds around each tin atom defines its formal charge by simply applying the octet rule. Thus, since tin is in group 14, a four-bonded tin atom will be neutral while a three-bonded tin atom carries a lone pair and therefore formal charge of 1-. This lead

to a charge of 44- for the cluster, that is, Sn_{56}^{44-} . The angles around the tin atoms are in the range 95.87(3)–114.83(2)°, with both extremes occurring at the four-bonded Sn_3 positions. This affirms that the dodecahedra are somewhat distorted and also indicates substantial strain at those four-bonded positions.

The cluster of Sn_{56} is endohedrally stabilized by four Ba^{2+} cations centered in each of the four dodecahedra (Figure 3). They reduce the overall formal charge of the cluster by eight, $[\text{Ba}_4@\text{Sn}_{56}]^{36-}$. If connected, the four Ba atoms form a tetrahedron at the vertexes of which the dodecahedra are positioned. Each cation has 19 rather than 20 tin neighbors (as for the pentagonal dodecahedron) because of the missing vertex that would have been common for the four dodecahedra. The distances to these neighbors range from 3.625(2) to 4.0797(8) Å (Table 3). It should be pointed out that these distances are very appropriate for Ba–Sn distances or, in other words, the barium cation fits very well in this cage. This can be illustrated by comparing the size of dodecahedral cavity, that is, the radius of the available empty space inside, 1.65 Å, with the radius of 12-coordinate (the maximum given in the literature) Ba^{2+} cation, 1.61 Å.⁹ The importance of such a good match between the “templating” cation and the cage size for the stabilization of a given structure has been discussed by us before.^{7,10} Apparently, the much smaller Ca^{2+} and Sr^{2+} are too small to fit well in a dodecahedron of tin since they do not form the corresponding isostructural compounds. Instead, they stabilize (endohedrally) the smaller clusters made of 12 tin atoms, (Sr or Ca)@ Sn_{12} with the shape of truncated tetrahedra, found in (Sr or Ca)@ $\text{Na}_{10}\text{Sn}_{12}$.⁵

Formations of fused dodecahedra are also found in other structures, specifically in the so-called intermetallic clathrates. The latter are three-dimensional structures made of four-bonded atoms of group 14 that form cages of various dimensions. These frameworks are stabilized by alkali or alkaline-earth metals that center the cages.^{10,11} One such structure is that of the clathrate of type II with stoichiometry $\text{A}_{24}\text{Tt}_{136}$ (Figure 4, top). Outlined with thick black lines in the figure is one such tetramer of fused dodecahedra, and the whole structure is made of such tetramers that are, in turn, fused to each other. This structure is analogous to the diamond structure since both crystallize in $Fd\bar{3}m$ and the tetramers of the clathrate occupy the carbon positions of the diamond. Thus, semiclose-packed layers perpendicular to the body diagonals can be identified in both structures. Larger cages made of 28 atoms (white in Figure 4, top) are formed between the fused dodecahedra. These large polyhedra are so large (when made of tin) that no single-atom cation in the periodic table is large enough to fit well inside. Thus, the clathrate-II structure is known for Si and Ge with sodium in the dodecahedra and rubidium or cesium in the 28-atom polyhedra, $(\text{Rb or Cs})_8\text{Na}_{16}(\text{Si or Ge})_{136}$, but is not known for tin.¹⁰ Instead, a reduced version of this structure is formed, $\text{A}_3\text{Na}_{10}\text{Sn}_{23}$ ($\text{A} = \text{K, Rb, Cs}$) with an average of -0.57 formal charge per tin atom compared to -0.18 in the clathrate-II composition.⁷ The size problem in this structure is solved very elegantly by separating the layers of fused pentagonal dodecahedra and filling the

(9) Shannon, R. D.; Prewitt, C. T. *Acta Crystallogr.* **1969**, B25, 925.

(10) (a) Bobev, S.; Sevov, S. C. *J. Am. Chem. Soc.* **1999**, 121, 3795. (b) Bobev, S.; Sevov, S. C. *J. Solid State Chem.* **2000**, 153, 92. (c) Bobev, S.; Sevov, S. C. *J. Am. Chem. Soc.* **2001**, 123, 3389.

(11) (a) Kasper, J. S.; Hagemuller, P.; Pouchard, M.; Cros, C. *Science* **1965**, 150, 1713. (b) Cros, C.; Pouchard, M.; Hagemuller, P. *Compt. Rend.* **1965**, 260, 4764.

(8) (a) Corbett, J. D.; Edwards, P. A. *J. Am. Chem. Soc.* **1977**, 99, 3313. (b) Fässler, T. F.; Hoffmann, S. Z. *Kristallogr.* **1999**, 214, 722 and references therein.

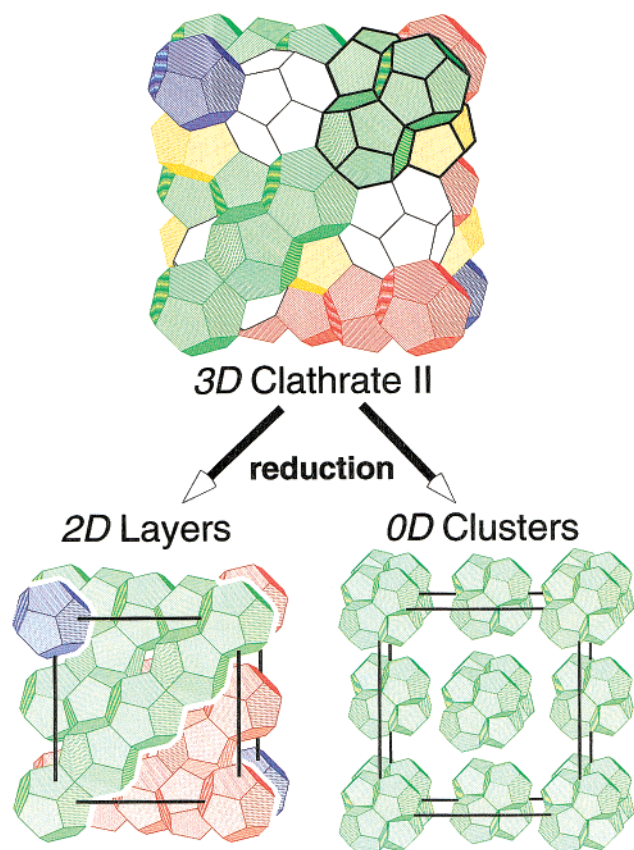


Figure 4. Shown are the relationships between the 3-D structure of clathrate II (top) and the structures of the reduced layered (2-D) clathrate-like $A_3Na_{10}Sn_{23}$ where $A = K, Rb, Cs$ (left),⁷ and the even more reduced naked 0-D clusters of Sn_{56} in $Ba_{16}Na_{204}Sn_{310}$ (right). Clathrate II is made of layers of fused pentagonal dodecahedra (the layers are shown in blue, green, and red), and larger polyhedra of 28 atoms (white) and other dodecahedra (yellow) are enclosed between those layers. The formations of four pentagonal dodecahedra as the clusters of Sn_{56} in $Ba_{16}Na_{204}Sn_{310}$ can be identified also in the clathrate-II structure where one of them is outlined with thick black lines (top).

interlayer space with more cations (Figure 4, left). This separation is possible thanks to the additional electrons from the extra cations which cleave the Sn–Sn bonds between the layers. In this light, the structure of $Ba_{16}Na_{204}Sn_{310}$ is a step further in reduction with -0.76 formal charge per tin atom. These additional electrons cleave more Sn–Sn bonds and reduce the dimensionality even further to zero-dimensional species, the isolated clusters of fused dodecahedra (Figure 4, right). The same tetramers of fused dodecahedra that exist as interconnected in clathrate II, are now separated from each other by the “electronic scissors”. They are now zero-dimensional clusters of 56 tin atoms that occupy all corners and face-centers of the cubic cell (Figures 1 and 4).

The Sn_{56} clusters can be considered also as indirectly related to fullerene cages that have been poked at four places, that is, concave fullerenes. They have 36 pentagonal faces rather than the 12 that are typical for normal fullerenes, and also, they do not have hexagonal faces. Like the carbon fullerenes Sn_{56} has three-bonded vertexes (Figure 2). However, it also has twelve four-bonded vertexes at the concave positions (Figure 2). These are the vertexes that are most likely responsible for the formation of this particular concave species. Since all vertexes of Sn_{56} are clearly sp^3 hybridized, the cluster is the sp^3 counterpart of the sp^2 -hybridized carbon fullerenes. Similarly hybridized but

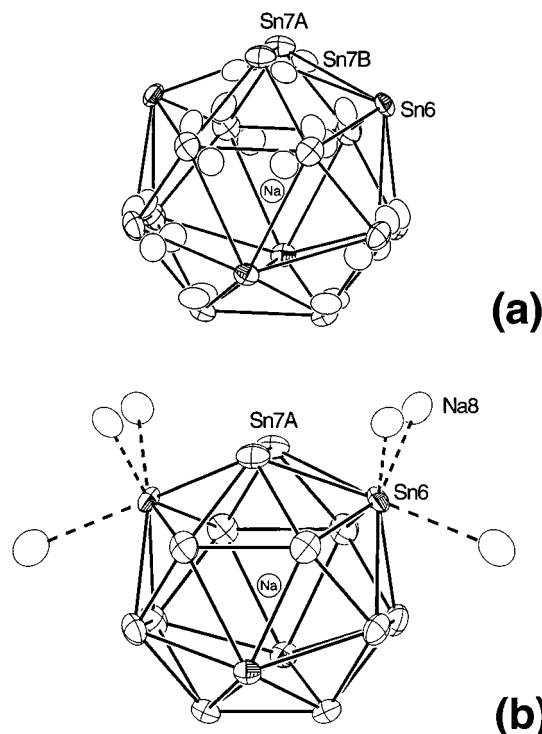


Figure 5. (a) Sn_{16-n} cluster with the shape of a capped truncated tetrahedron (50% ellipsoids). The capping atoms, Sn6, are partially occupied so that there are Sn_{16} , Sn_{15} , Sn_{14} , Sn_{13} , and Sn_{12} species in the structure. The Sn7 position that forms the truncated tetrahedron was refined as a split position of Sn7A (crossed ellipsoids) and Sn7B (open ellipsoids). Sn6 can be bonded only to Sn7A (shown) since the distances to Sn7B are too short. The cluster is centered by a sodium cation. (b) ORTEP view of the Sn_{16-n} cluster (60% thermal ellipsoids, the positions Sn7B are not shown) with the nearest sodium neighbors. Sn6 has three sodium cations as near *exo*-neighbors at distances of 3.02(1) Å (Table 3). When Sn6 is missing, these three sodium atoms cap the open hexagonal face made of Sn7B with distances 3.06(2) Å.

fused fullerene-like species are known for indium and aluminum as well.¹² In analogy with the hydrocarbons, it has been proposed that the sp^3 -hybridized clusters could be called *fullerenes* since the sp^2 species are *fullerenes*.^{12b,c}

The novel phase $Ba_{16}Na_{204}Sn_{310}$ exhibits two additional structural features, deltahedra of $(16-n)$ atoms stabilized interstitially by sodium cations, and *arachno*-deltahedra of 8 atoms (Figures 1, 5, and 6). The geometry of the former is of a capped truncated tetrahedron, often referred to as Franck–Kasper polyhedron (Figure 5).^{1c} The position that forms the truncated tetrahedron (initially found with a very long thermal ellipsoid) was refined as a split position of Sn7A and Sn7B (0.67 Å apart) that sum to a full occupancy in approximately 3:1 ratio (Figure 5). Thus, the truncated tetrahedra themselves are complete, that is, without defects. The capping position, Sn6, however, was refined at close to 40% occupancy in the four different refinements, and this partial occupancy makes uncertain the number of vertexes per cluster, that is, Sn_{16-n} . It means that there are clusters of different sizes: Sn_{16} , Sn_{15} , Sn_{14} , Sn_{13} , and Sn_{12} for 0, 1, 2, 3, and 4 missing Sn6 atoms, respectively. The first four clusters are deltahedral species with delocalized bonding while Sn_{12} is made of tin atoms that are 3-bonded with “normal” localized 2-center-2-electron bonds. The charge of the

(12) (a) Sevov, S. C.; Corbett, J. D. *Science* **1993**, 262, 880. (b) Sevov, S. C.; Corbett, J. D. *J. Solid State Chem.* **1996**, 123, 344. (c) Nesper, R. *Angew. Chem., Int. Ed. Engl.* **1994**, 33, 843.

latter is therefore 12^- , that is, Sn_{12}^{12-} . Exactly the same cluster with the same charge has been found in $(\text{Ca or Sr})\text{Na}_{10}\text{Sn}_{12}^{5-}$ *closo*-Deltahedra with the shape of tetracapped truncated tetrahedra, that is, species such as Sn_{16} , are known to require 68 electrons for bonding (includes the cluster-bonding electrons and the electrons for the 16 electron pairs at the vertexes).¹³ This means that the charge for the tin cluster will be 4^- , that is, Sn_{16}^{4-} , since 16 tin atoms provide $16 \times 4 = 64$ electrons. Furthermore, it is also known that removal of a vertex increases the charge by 2, that is, Sn_{15}^{6-} , Sn_{14}^{8-} , and Sn_{13}^{10-} .¹⁴ Thus, we could have clusters with the following sizes and charges: Sn_{16}^{4-} , Sn_{15}^{6-} , Sn_{14}^{8-} , Sn_{13}^{10-} , and Sn_{12}^{12-} for missing 4-, 3-, 2-, 1-, and 0-capping Sn_6 atoms. Clearly the negative charge of the clusters increases by two for each missing capping atom or, in other words, can be given as $\text{Sn}_{16-n}^{(4+2n)-}$. The overall occupancy of 40% for the Sn_6 site translates into an average of 1.5(1) capping atoms per cluster or, in other words, the average size of the cluster is 13.5(1) atoms. This size defines the average charge of -9 per cluster throughout the structure, $\text{Sn}_{13.5}^{9-}$. This, of course, is just the average size and charge, while the structure contains species perhaps of all the sizes given above.

The distances from the capping Sn_6 site to the split positions $\text{Sn}7\text{A}$ and $\text{Sn}7\text{B}$ are quite different, 3.273(2) and 2.77(1) Å, respectively, which indicates that when the capping site is occupied the $\text{Sn}7\text{B}$ position is empty, due to the impossibly short distance (Figure 5a). On the outside, this capping position Sn_6 is surrounded by three sodium cations at distances of 3.02-(1) Å (Figure 5b). These cations cap three of the triangular faces made of Sn_6 and two $\text{Sn}7\text{A}$ when the capping atom is present. When it is missing, on the other hand, the open hexagonal face is made of $\text{Sn}7\text{B}$, and the same three sodium cations cap that face with distances of 3.06(2) Å to $\text{Sn}7\text{B}$. Thus, there is no “vacuum” left anywhere throughout the structure. It seems that the disorder between $\text{Sn}7\text{A}$ and $\text{Sn}7\text{B}$ is caused by the partial occupancy of the capping position Sn_6 since two different sites are needed for occupied and empty Sn_6 position. The $\text{Sn}_{13.5}^{9-}$ cluster is centered by a sodium cation with distances to the cage atoms in the range 3.18(1)–3.369(2) Å (Figure 5). It reduces the charge of the overall cluster by one, $[\text{Na}@\text{Sn}_{13.5}]^{8-}$. The clusters occupy the center of the cubic cell and the centers of all of its edges, that is, all octahedral holes of the face-centered lattice made of the Sn_{56} clusters (Figure 1).

The third feature in the structure of $\text{Ba}_{16}\text{Na}_{204}\text{Sn}_{310}$ is a cluster that occupies half of the tetrahedral holes in the lattice, the ones at the $\bar{4}3m$ position of $1/4, 1/4, 1/4$ (Figures 1 and 6), that is, there are four of these clusters per cell, the same as for Sn_{56} and Sn_{16-n} . The refinement of this cluster and the recognition of its type were the most troublesome steps in the structure determination. The cluster appears as a nearly spherical shell of very diffuse and continuous electron density without well defined maxima (Figure 6a). This density was fitted with three independent tin atoms (16-fold Sn_8 and Sn_9 , and 96-fold Sn_{10}) with unreasonably short distances between some of their symmetry-equivalent positions. They refined as partially occupied and with extremely anisotropic and large thermal ellipsoids in the shape of two-dimensional tangential disks. These disks cover almost the whole sphere with only a few

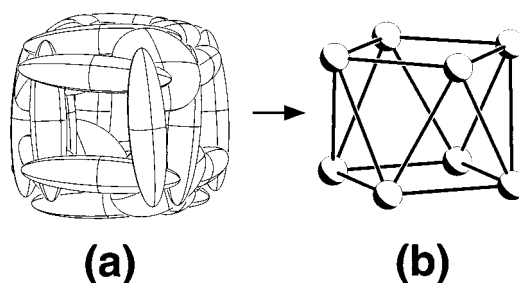


Figure 6. Disordered Sn_8 cluster: (a) an ORTEP plot (90% probability thermal ellipsoids) of the overall electron density of the cluster with all symmetry equivalent positions shown, and (b) one of the many positions of the square antiprism as resolved from the disorder.

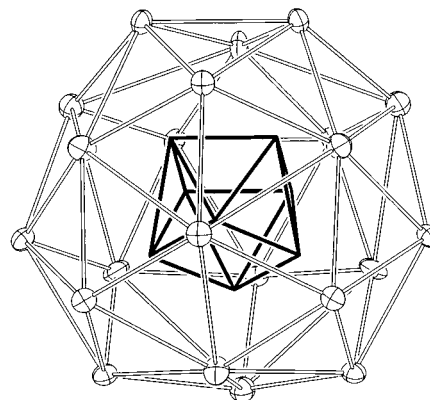


Figure 7. View of the positioning of the highly symmetric (T_d) Na_{22} cage (30% probability thermal ellipsoids) around one of the orientations of the disordered *arachno*- Sn_8 cluster (D_{4d}). Since the cluster is of lower symmetry, it can take many different orientations with respect to the cage that would be indistinguishable in terms of energy or occupation of space.

electron density-free spots (Figure 6a). However, the sum of the occupancies of these atoms added up to exactly 8.0(2) atoms per cluster for all four refinements. This knowledge combined with the knowledge of the shape of the Sn_8 clusters characterized (thoroughly) in $\text{A}_4\text{Li}_2\text{Sn}_8$ ($\text{A} = \text{K}, \text{Rb}$)³ and a careful look at the positioning of the centers of the ellipsoids revealed that the real cluster is most likely a square antiprism (Figure 6b) of tin that is highly disordered between many different orientations throughout the structure. The Sn – Sn distances in the square antiprism are within the range 2.729(5)–3.10(2) Å. The lower end of this range is somewhat too short for such distance, but for atoms refined with such anisotropic thermal ellipsoids, this is not unexpected. The disorder of the cluster is possible because of the higher symmetry of the surrounding “cage” of sodium cations which defines the local symmetry as $\bar{4}3m$, that is, the maximum point symmetry for this space group (Figure 7). Such disorder is quite common for similar systems with species of lower symmetry that are inside a cavity of higher symmetry because this allows the inside formation to take many different orientations with respect to the cavity that are indistinguishable in terms of energy or occupation of space.¹² For example, similarly disordered Ni-centered 10-atom clusters of indium with approximate symmetry C_{3v} , $[\text{In}_{10}\text{Ni}]$, were encountered in the structures of $\text{Na}_{96}\text{In}_{\sim 97}\text{Ni}_2$ and $\text{Na}_{\sim 172}\text{In}_{\sim 197}\text{Ni}_2$ where they reside inside fullerene-like cages of In_{60} and In_{74} with much higher symmetry. In the case of $\text{Ba}_{16}\text{Na}_{204}\text{Sn}_{310}$ the Sn_8 cluster is of D_{4d} symmetry while the outside cage is of the much higher T_d symmetry. This leads to a condition that can be described as angular incommensurability.

(13) Sevov, S. C.; Corbett, J. D. *Inorg. Chem.* **1992**, *31*, 1895.

(14) Wade, K. *Adv. Inorg. Chem. Radiochem.* **1976**, *18*, 1.

It should be pointed out that reported recently was a cluster of tin of exactly the same shape, a square antiprism, in the compound $A_4Li_2Sn_8$ for $A = K, Rb$.³ Such shape corresponds to an *arachno*-deltahedron derived from the corresponding *closo*-shape of a bicapped square antiprism after removing the two capping vertexes. Thus, based on Wade's rules for counting electrons in such deltahedral species the *arachno*-cluster has a charge of -6 , that is, Sn_8^{6-} .³ For comparison, the Sn–Sn distances of the cluster in $A_4Li_2Sn_8$ range from 2.947(3) to 3.044(2) Å, and except the lower end are not too far from those of Sn_8 in $Ba_{16}Na_{204}Sn_{310}$ (above).

The overall composition of the unit cell of the new compound is thus made of four of each of the three different clusters $[Ba_4@Sn_{56}]^{36-}$, $[Na@Sn_{13.5}]^{8-}$, and $[Sn_8]^{6-}$ and 200 sodium cations, $Na_{200}([Ba_4@Sn_{56}]^{36-})[Na@Sn_{13.5}]^{8-}[Sn_8]^{6-})_4$. Of course, the partially occupied cluster with an average formula $[Na@Sn_{13.5}]^{8-}$ will be represented by the corresponding species with 0 to 4 missing capping atoms (see above) but in such a ratio as to give this average formula and charge. In this formula the total negative charge of -200 is balanced by the 200 sodium cations. However, deviations from this “ideal” stoichiometry are possible, in particular the occupancy of Sn_6 . This leads to temperature-independent magnetic susceptibility that is very close to zero but is unclear whether it is slightly positive as in metals or slightly negative as in insulators.

Conclusions

$Ba_{16}Na_{204}Sn_{310}$ is a compound with a very complex structure where space is filled with three different anionic species of different sizes, Sn_{56} , Sn_{16-n} , and Sn_8 , that are packed with much smaller cations of sodium. The mismatch, clearly demonstrated in the disorder of Sn_8 and the partially occupied Sn_{16-n} , is not surprising. What is surprising is that it is possible at all, that is, that somehow balance between packing efficiency, electronic requirements, and covalent interactions has been found. It illustrates the power of combining cations of different sizes as well as charges. One can envision removal of the disorder by substitution at some tin sites and thus changing the number of required cations in a yet-to-be-found compound.

Acknowledgment. We thank the National Science Foundation (CHE-0098004) and the donors of the Petroleum Research Fund administered by the ACS for support of this research.

Supporting Information Available: An X-ray crystallographic file for the structure of $Ba_{16}Na_{204}Sn_{310}$ (four refinements) in CIF format. This material is available free of charge via the Internet at <http://pubs.acs.org>.

JA012549J